# SIMULASI BERANGKA PEROLAKAN BEBAS BAHANTARA BERLIANG BERSIMETRI PAKSI

*NUMERICAL SIMULATION FOR FREE CONVECTION IN AXISYMMETRIC POROUS MEDIUM*

Oleh

CHAN KIEN WING

65395

Penyelia

ASSOC. PROF. PA ASWATHA NARAYANA

February 2005

Disertai ini dikemukakan kepada

Universiti Sains Malaysia

Sebagai memenuhi sebahagian daripada syarat untuk pengijazahan dengan kepujian

**SARJANA MUDA KEJURUTERAAN MEKANIK**


Pusat Pengajian Kejuruteraan Mekanik

Kampus Kejuruteraan

Universiti Sains Malaysia

## DECLARATION

This work has not previously been accepted in substance for any degree and is not being concurrently submitted in candidature for any degree.

Signed ……..…. (candidate)
Date …….....

STATEMENT 1

This thesis is the result of my own investigations, except where otherwise stated. Other resources are acknowledged by giving explicit references. A bibliography/references are appended.

Signed ……..…. (candidate)
Date …….....

STATEMENT 2

I hereby give consent for my thesis, is accepted, to be available for photocopying and for interlibrary loan, and for the title and summary to be made available to outside organizations.

Signed ……..…. (candidate)
Date …….....

# ACKNOWLEDGEMENT

First and foremost, I would like to thank my project supervisors, **Assoc. Prof P. A. Aswatha Narayana** and **Assoc. Prof. Dr. Haji Zainal Alimuddin b. Zainal Alauddin** who guided me in accomplishing this project.. They have been supporting me to make this project a success.

Thanks to Irfan and Raju who gave constructive suggestions and comments during my project. They had inspired me indirectly and made lot of contributions. It is my great pleasure to have them as friends.

Finally, my final year project had been finished with great joy and satisfactory.

I wish to express my thanks to my dear parents who gave me encouragement and support financially and emotionally. Their words of encouragement have been a great treasure during the time I faced obstacles and difficulties.

# CONTENTS

# LIST OF FIGURES

## NOMENCLATURE

| | |
|---|---|
| $A^*$ | aspect ratio |
| $r^*$ | radius ratio |
| $T$ | temperature |
| $T_i$ , $T_o$ | inner and outer wall temperature |
| $r_i$ , $r_o$ | inner and outer radius |
| $H$ | height of axisymmetric porous medium |
| $\psi$ | streamline function |
| $\mu$ | viscosity |
| $\nu$ | kinematics viscosity |
| $u$, $v$, $w$ | velocity in $r$, $\theta$, and $z$ directions |
| $\rho$ | density |
| $\beta$ | thermal expansion |
| $\alpha$ | thermal diffusivity |
| K | permeability |
| $\overline{R}$ | average radius of an element |
| $N_1$ , $N_2$ , $N_3$ | shape functions for the triangular element |
| $p$ | pressure |

# ABSTRAK

Kaedah berangka unsur terhingga dengan mengaplikasi kaedah *Galerkin* telah digunakan untuk analisa pemindahan haba dalam bahantara berliang bersimetri paksi secara perolakan bebas. Cara ini telah digunakan untuk mengkaji kesan nisbah aspek (0.6 – 8) dan nisbah jejari (0.1 – 10) terhadap purata nombor *Nusselt*. Kesan nombor *Rayleigh* antara 10 – 100 terhadap purata nombor Nusselt juga diambil kira dalam kajian.

Tiga kes dikaji di sini: dinding sesuhu, perubahan suhu secara penguasan samada dinding luaran atau dalaman dan perolakan bebas pada dinding dalaman. Indek kuasa yang dikaji ialah antara 0.25 – 1.00. Dengan dinding luaran yang dikenakan pada perolakan bebas, koefisien haba pemindahan antara 0.01 – 100 telah disiasat kesannya terhadap purata nombor *Nusselt* juga.

# ABSTRACT

Computational finite element method employing Galerkin's method of weighted residuals has been used to analyze free convection heat transfer in axisymmetric porous medium saturated by fluid. The approach is used to study the effect of aspect ratio (0.6 – 8), radius ratio (0.1 – 10) and Rayleigh number range from 10 – 100 on the average Nusselt number, $\overline{Nu}$ in the case of porous cylindrical annulus.

Three cases are studied here: isothermal wall temperature, power law temperature variation on both inner or outer wall and convective boundary on outer wall. The power law index for the power law temperature variation is ranges from 0.25 – 1.00. With convective boundary at the outer wall of the axisymmetric porous medium, heat transfer coefficient of 0.01 – 100 ($W/m^2.K$) is taken into the study for the effect on the average Nusselt number.

# Chapter 1 INTRODUCTION

Vertical porous enclosures with axisymmetrical geometry are always encountered in many engineering applications. Its wide applications include geothermal energy engineering, groundwater pollution transport, nuclear waste disposal, chemical reactors engineering, insulation of buildings and pipes, and storage of grain and coal, and so on.

The study of heat transfer of porous medium has, in recent past, become a matter of considerable importance and interest because of the growing demand for energy, environment, comfort, safety, and advanced materials. Heat transfer is concerned with the physical processes underlying the transport of thermal energy due to a temperature difference or gradient. The efficiency of a system involving porous medium, such as electronic component is also a strong function of the heat transfer to and from various components of the system. All these considerations make it imperative to obtain accurate, consistent, and physically valid results on the heat transfer to relate these to the design, control, and optimization of the system.

There has been a phenomenal increase in the use of computational methods for engineering applications in recent years. This is particularly true for problems in heat transfer and fluid flow, since the complexity of the governing equations generally allows analytical solutions to be obtained for very simple cases, making it necessary to use numerical technique for most problems of practical interest. Here for the free convection of axisymmetric porous medium, the finite element method has been used.

The finite element method is based on various integral formulations of the conservation principles. The region under study is divided into a number of finite elements, these element being of various shapes. The integral statement of the governing conservation postulates yield the integral equations that apply for each element. The integrals are reduced by weighted residuals method. The method of weighted residuals is an approximate technique for solving boundary value problems that utilizes trial function satisfying prescribed boundary conditions and an integral formulation to minimize error.

Some commercially available software, such as Maple, Mathematica, Macsyma, and MathCAD, employ symbolic processing software capable of doing algebra, calculus,

and other mathematical operations symbolically, rather than numerically, to obtain analytical solutions whenever possible. An environment which is very convenient to use is provided by Matlab, which has extensively used computational software for solving mathematical problems of engineering interest. Because of its convenient user interface, visualization capability, programmability, and wide range of techniques and command, Matlab has become a computational tool in analysis the free convection of axisymmetric porous medium.

Knowledge of the variation of heat transfer with radius and respect ratio would be very useful in determining the optimum insulation thickness for porous medium application. By applying the available source codes with the use of MATLAB, the temperature and stream function variations can easily be determined.

# Chapter 2 LITERATURE REVIEW

Flow and heat transfer in fluid saturated porous medium are being studied and have become interesting for researcher. This research is crucial because of their natural occurrence and its importance in industrial applications. The development of Darcy's phenomenological relation in 1856 was the starting point for research on porous media flow. Darcy's relation gives good solution for solving porous media problems like flow in a soil medium when it is less porous. Many of the porous medium application in industries require knowledge of porous medium behavior to ensure the products are reliable and compatible. In many common situations, many critical problems occurred for the product design using porous materials. To overcome these problems, the researchers used the experimental and numerical analysis to predict the behavior of the porous material. Researchers produced a contemporary literature on porous media showing that the combined flow and thermal problem is still a very active area of research.

In a review article, Cheng (1978) enlisted the various cases of heat transfer by free and mixed convection into porous medium while J.J Shu and I Pop (1999) elaborately discussed on the topic of free convection and forced convection in porous medium. The dissertation by Rajamani (1989), Satya Sai (1993), Partiban (1995) and Nithiarasu (1996) provides a comprehensive review of earlier and on going research activity in this field. In addition to this, a number of research papers on heat and mass transfer are available to indicate the importance of porous media application in daily use.

The thermal convection is described as an energy transfer process occurring in between solid surface and liquid by means of the combined action of heat conduction and fluid motion. There are two types of thermal convection which are free and force convection when the fluid is in contact with the body. In natural convection, the motion of the fluid particles in contact with a solid surface is generated due to the energy transferred by conduction from the solid surface. Natural convection in a single phase fluid can also be treated as a limiting case of the porous medium flow when porosity equals to 1 and permeability value approaching infinity. Even though laminar natural convection in a single-phase fluid has been studied well in literature, it is essential to

understand the type of flow pattern and heat transfer, before dealing with porous media problem. An excellent introduction to the subject is given by Ostrach (1988) with new developments in the area of natural convection heat transfer. In this review article, there are some experimental investigations presented relating to natural convection from the vertical and horizontal plate. Later, the energy conservation in single-phase fluid has been formulated for theoretical study based on experimental investigations.

Laminar natural convection heat transfers in tall enclosures have been studied experimentally and numerically by Elder (1965). At high Rayleigh numbers multi-cellular patterns were observed. The porous media theoretical analyses have been solved by Tabbarok and Lin (1977) by using finite element method to simplify the complexity of natural convection heat transfer model. Nath and Satyamurthy (1985) have used a finite difference method to evaluate the variation of Nusselt number with aspect ratio, radius ratio and Rayleigh number. Satya Sai (1993) studied the effect of radius ratio on natural convection heat transfer in an annular enclosure applying the finite element method.

From the application perception, convection in complicated geometry such as rectangular and cylindrical shapes of cavities is of practical importance. The numerical analysis is being used because it requires less time and increases the computational power to predict the flow regime when compared with experimental analysis. Vertical porous enclosure with cylindrical geometry is encountered by Nath and Satyamurthy (1985) whereas they have used finite difference method to evaluate the variation of Nusselt Number with aspect ratio, radius ratio and Rayleigh number. They have given results in the range of $50< Ra<500$; $0.2<A^*<8$ and $0.25<r^*<8$. Very few studies have been carried out in finding the effect of above parameters on Nusselt number. Prasad and Kullacki (1984) carried out a study of curvature effects on temperature and velocity fields in a vertical porous annulus. They considered a wide range of Rayleigh numbers up to 10,000.

The Galerkin's finite element method was used by Hickox and Gartling (1985) to solve the natural convective heat transfer in axisymmetric porous cavity. From the results, the heat transfer rate has been observed to increase about 2.6 times in the presence of convection when compared to the pure thermal conduction. Later Rajamani et al. (1995) used the same approach to study the effect of aspect ratio and radius ratio on Nusselt

number in the case of a porous cylindrical annulus. It is seen that the maximum average Nusselt number when the aspect ratio is around unity.

From the literature review, it has been seen that, most of the researchers employed analytical solution to predict the behavior of the porous medium. The analytical solution in nature compared well with the experimental results. Hence analytical approach has becomes a foundation to the researchers to justify the applications in nature. Finite element method has in a simplified manner been used in the present work to analyze the problem. This method has a strong computational power and it is applicable for analysis of arbitrary shaped studies.

# Chapter 3 METHODOLOGY

A cylindrical, saturated porous annulus of inner radius, $r_i$ and outer radius, $r_o$ is to be used. Since the body is axisymmetric, two coordinates $r$ and $z$ are sufficient to describe the system completely.

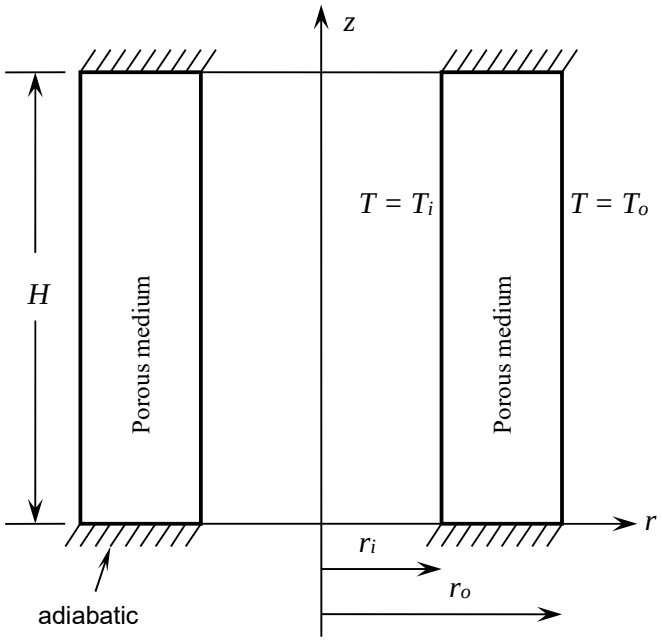


**Figure 3.1**: Coordinate system and geometry

Assumptions:

(i) The porous medium considered is saturated by fluid.

(ii) The porous medium is homogeneous and isotropic.

(iii) Fluid properties are constant except density variation which produces a buoyancy force.

(iv) The fluid and porous medium is everywhere in local thermodynamic equilibrium.

(v) Additional viscous and inertial terms are, for low Darcy number, neglected because of their small magnitudes compared to other terms.

(vi) Dispersion and radiation effects are neglected..

The non-dimensional cylindrical coordinates is being used here for single phase fluid. The non-dimensional variables used in cylindrical coordinates system are:

$$\bar{r} = \frac{r}{L_{ref}}, \qquad \bar{z} = \frac{z}{L_{ref}}, \qquad \bar{\psi} = \frac{\psi}{\alpha_f L_{ref}}, \quad \bar{T} = \frac{(T - T_{cold})}{(T_{hot} - T_{cold})} \tag{3.1}$$

Under the above assumption, the governing equations in cylindrical coordinates are written as (Srinivas[11], 1989):

Continuity equation:

$$\frac{\partial(ru)}{\partial r} + \frac{\partial(rw)}{\partial z} = 0 \tag{3.2}$$

Darcy's law in the r direction:

$$u = -\frac{K}{\mu}\frac{\partial p}{\partial r} \tag{3.3}$$

Darcy's law in the z direction:

$$w = -\frac{K}{\mu}\left(\frac{\partial p}{\partial z} + \rho g\right) \tag{3.4}$$

Energy equation:

$$u\frac{\partial T}{\partial r} + w\frac{\partial T}{\partial z} = \alpha\left(\frac{1}{r}\frac{\partial}{\partial r}\left(r\frac{\partial T}{\partial r}\right) + \frac{\partial^2 T}{\partial z^2}\right) \tag{3.5}$$

Equation of state:

$$\rho = \rho_\infty(1 - \beta(T - T_\infty)) \tag{3.6}$$

We introduce the stream function $\psi$ defined by (Bejan[8], 1984),

$$u = -\frac{1}{r}\frac{\partial \psi}{\partial z} \tag{3.7}$$

$$w = \frac{1}{r}\frac{\partial \psi}{\partial r} \tag{3.8}$$

The continuity equation is automatically satisfied by the introduction of the $\psi$. One governing equation is thus eliminated.

Eliminating the variable $p$ from (3.3) and (3.4) and incorporating $\psi$ we obtain,

$$\frac{\mu}{K}\frac{1}{r}\left(\frac{\partial^2 \psi}{\partial r^2} + \frac{\partial^2 \psi}{\partial z^2}\right) + \frac{1}{r^2}\frac{\mu}{K}\frac{\partial \psi}{\partial r} = \rho_\infty \beta g \frac{\partial T}{\partial r} \tag{3.9}$$

Using $\nu = \mu / \rho$, we obtain,

$$\frac{\partial^2 \psi}{\partial z^2} + \frac{1}{r}\frac{\partial}{\partial r}\left(r\frac{\partial \psi}{\partial r}\right) = r\frac{\mathrm{K}g\beta}{\nu}\frac{\partial T}{\partial r} \tag{3.10}$$

Substituting *u* and *w* in terms of $\psi$ in (3.5), we obtain,

$$\alpha\left(\frac{1}{r}\frac{\partial}{\partial r}\left(r\frac{\partial T}{\partial r}\right) + \frac{\partial^2 T}{\partial z^2}\right) = -\frac{1}{r}\frac{\partial \psi}{\partial z}\frac{\partial T}{\partial r} + \frac{1}{r}\frac{\partial \psi}{\partial r}\frac{\partial T}{\partial z} \tag{3.11}$$

Equations (3.10) and (3.11) are the two governing equations to be formulated into finite element matrix equations. Each equation has both the variables $\psi$ and *T*, we thus have two coupled equations which have to be solved simultaneously.

The simplex 3 nodes triangular element is used for the analysis. The variation of temperature T and $\psi$ inside the element are given by,

$$\begin{aligned} T &= N_1 T_1 + N_2 T_2 + N_3 T_3 \\ &= [\,N\,]\,\{\,T\,\} \end{aligned} \tag{3.12}$$

$$\begin{aligned} \psi &= N_1 \psi_1 + N_2 \psi_2 + N_3 \psi_3 \\ &= [\,N\,]\,\{\psi\} \end{aligned} \tag{3.13}$$

where $N_1$, $N_2$, $N_3$ are the shape function given by,

$$N_i = \frac{a_i + b_i r + c_i z}{2A} \qquad i = 1, 2, 3 \tag{3.14}$$

Using Galerkin's method, (3.10) becomes,

$$\int_V N^T\left(\frac{\partial^2 \psi}{\partial z^2} + \frac{1}{r}\frac{\partial}{\partial r}\left(r\frac{\partial \psi}{\partial r}\right) - r\frac{\mathrm{K}g\beta}{\nu}\frac{\partial T}{\partial r}\right)dV = 0 \tag{3.15}$$

where $dV = 2\pi\, r\, \mathrm{d}r\, \mathrm{d}z$ for axisymmetric geometries.

Integration of first two terms gives (Srinivas[11], 1989),

$$\int_V N^T\left(\frac{\partial^2 \psi}{\partial z^2} + \frac{1}{r}\frac{\partial}{\partial r}\left(r\frac{\partial \psi}{\partial r}\right)\right)2\pi r\, dr\, dz =$$

$$\frac{2\pi \bar{R}}{4A}\left[\begin{bmatrix} b_1^2 & b_1 b_2 & b_1 b_3 \\ b_1 b_2 & b_2^2 & b_2 b_3 \\ b_1 b_2 & b_2 b_3 & b_3 \end{bmatrix} + \begin{bmatrix} c_1^2 & c_1 c_2 & c_1 c_3 \\ c_1 c_2 & c_2^2 & c_2 c_3 \\ c_1 c_2 & c_2 c_3 & c_3 \end{bmatrix}\right]\begin{Bmatrix} \psi_1 \\ \psi_2 \\ \psi_3 \end{Bmatrix} \tag{3.16}$$

The third term in the parenthesis is,

$$\int N^T \left( \frac{\mathrm{K}g\beta}{\nu} r \frac{\partial T}{\partial r} \right) 2\pi r \ \mathrm{d}r \, \mathrm{d}z = 2\pi \bar{R}^2 \frac{\mathrm{K}g\beta}{6\nu} \begin{Bmatrix} b_1T_1 + b_2T_2 + b_3T_3 \\ b_1T_1 + b_2T_2 + b_3T_3 \\ b_1T_1 + b_2T_2 + b_3T_3 \end{Bmatrix} \tag{3.17}$$

The solution for the governing equation of (3.15) by using finite element method is given as

$$\frac{2\pi \bar{R}}{4A} \left[ \begin{bmatrix} b_1^2 & b_1b_2 & b_1b_3 \\ b_1b_2 & b_2^2 & b_2b_3 \\ b_1b_2 & b_2b_3 & b_3 \end{bmatrix} + \begin{bmatrix} c_1^2 & c_1c_2 & c_1c_3 \\ c_1c_2 & c_2^2 & c_2c_3 \\ c_1c_2 & c_2c_3 & c_3 \end{bmatrix} \right] \begin{Bmatrix} \psi_1 \\ \psi_2 \\ \psi_3 \end{Bmatrix} = -2\pi \bar{R}^2 \frac{Kg\beta}{6\nu} \begin{Bmatrix} b_1T_1 + b_2T_2 + b_3T_3 \\ b_1T_1 + b_2T_2 + b_3T_3 \\ b_1T_1 + b_2T_2 + b_3T_3 \end{Bmatrix} \tag{3.18}$$

Similarly, use Galerkin's method for (3.11) yields,

$$\int N^T \left[ \alpha \frac{1}{r} \frac{\partial}{\partial r} \left( r \frac{\partial T}{\partial r} \right) + \alpha \frac{1}{r} \frac{\partial^2 T}{\partial z^2} + \frac{1}{r} \frac{\partial \psi \partial T}{\partial z \partial r} - \frac{1}{r} \frac{\partial \psi \partial T}{\partial r \partial z} \right] 2\pi r \ dr \, dz = 0 \tag{3.19}$$

Integrating, the first two terms in the parenthesis become,

$$\int N^T \left[ \alpha \frac{1}{r} \frac{\partial}{\partial r} \left( r \frac{\partial T}{\partial r} \right) + \alpha \frac{1}{r} \frac{\partial^2 T}{\partial z^2} \right] 2\pi r \, dr \, dz =$$

$$\frac{2\pi \bar{R}\alpha}{4A} \begin{bmatrix} b_1^2 & b_1b_2 & b_1b_3 \\ b_1b_2 & b_2^2 & b_2b_3 \\ b_1b_3 & b_2b_3 & b_3^2 \end{bmatrix} \begin{Bmatrix} T_1 \\ T_2 \\ T_3 \end{Bmatrix} + \frac{2\pi \bar{R}\alpha}{4A} \begin{bmatrix} c_1^2 & c_1c_2 & c_1c_3 \\ c_1c_2 & c_2^2 & c_2c_3 \\ c_1c_3 & c_2c_3 & c_3^2 \end{bmatrix} \begin{Bmatrix} T_1 \\ T_2 \\ T_3 \end{Bmatrix}$$

$$+ \frac{2\pi h L_{jk}}{12} \begin{bmatrix} 0 & 0 & 0 \\ 0 & 3R_j + R_k & R_j + R_k \\ 0 & R_j + R_k & R_j + 3R_k \end{bmatrix} - \frac{2\pi h L_{jk} T_\infty}{6} \begin{Bmatrix} 0 \\ 2R_j + R_k \\ R_j + 2R_k \end{Bmatrix} \tag{3.20}$$

where *jk* is the side along which the convection boundary condition exists.

$$\int_V N^T \frac{1}{r} \frac{\partial \psi}{dz} \frac{\partial T}{dr} dV = \frac{2\pi}{12A} \begin{bmatrix} c_1\psi_1 + c_2\psi_2 + c_3\psi_3 \\ c_1\psi_1 + c_2\psi_2 + c_3\psi_3 \\ c_1\psi_1 + c_2\psi_2 + c_3\psi_3 \end{bmatrix} \begin{bmatrix} b_1 & b_2 & b_3 \end{bmatrix} \begin{Bmatrix} T_1 \\ T_2 \\ T_3 \end{Bmatrix} \tag{3.21}$$

$$\int_V N^T -\frac{1}{r} \frac{\partial \psi}{dz} \frac{\partial T}{dr} dV = -\frac{2\pi}{12A} \begin{bmatrix} b_1\psi_1 + b_2\psi_2 + b_3\psi_3 \\ b_1\psi_1 + b_2\psi_2 + b_3\psi_3 \\ b_1\psi_1 + b_2\psi_2 + b_3\psi_3 \end{bmatrix} \begin{bmatrix} c_1 & c_2 & c_3 \end{bmatrix} \begin{Bmatrix} T_1 \\ T_2 \\ T_3 \end{Bmatrix} \tag{3.22}$$

Equations (3.16) through (3.22) yield two simultaneous matrix equations for an element. These matrix equations are assembled to obtain the total matrix equations for the domain. Initially the value of $\psi$ is taken to be zero for the first iteration. The value of $\{T\}$ obtained by solving the first set of equations are then used to solve the second set of global matrix equations. These values of $\{\psi\}$ are then used for the next iteration in calculation of $\{T\}$. The two equations are thus solved by iteration. For the solution to converge it is necessary that a fine mesh is used.

Figure 3.1 shows the cross section of a cylindrical annulus with cylindrical coordinates. The remaining two horizontal walls are considered as adiabatic. Both sides of the annulus are symmetrical. Hence right side of the cross section of axisymmetric porous medium is sufficient for the numerical analysis. Further the heat transfer coefficients can be multiplied by area of the cylinder to obtain the total heat transfer rate. Before the numerical analysis, the region of height $H$ and breadth $(r_0 - r_i)$ is discretized into linear triangular elements with fine mesh near the four bounded walls.

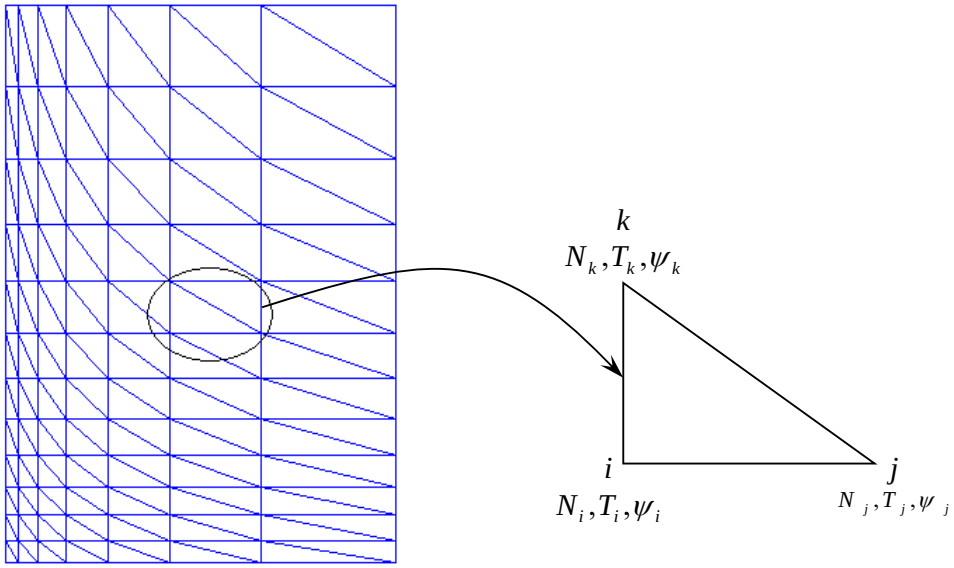


**Figure 3.2**: A linear three nodded triangular element

These algebraic equations are coded in a Matlab program to solve for the temperature and stream functions at various boundary conditions applied.

From the finite element method (FEM) analysis for various parameters such as aspect ratio, radius ratio and Rayleigh numbers are used to obtain the respective average Nusselt number values.

Aspect ratio $A^*$ for the cylinder is defined as:

$$A^* = \frac{H}{L}$$

whereas the radius ratio $r^*$ is defined as:

$$r^* = \frac{(r_0 - r_i)}{r_i}$$

The Rayleigh number in the present case is defined as (Bejan[8], 1984):

$$Ra = \frac{Kg\beta(T_1 - T_0)L}{\nu\alpha} \tag{3.23}$$

where $L = r_0 - r_i$

The boundary conditions of $u = 0$ at $r = r_i$ and $r = r_o$ and $w = 0$ at $z = 0$ and $z = H$ are incorporated by forcing $\psi$ to be zero on all four boundaries. The temperatures on the two vertical walls are forced to be:

(a) Isothermal where $T_i > T_o$

(b) $T_i(z) = T_o + Az^{\lambda}$ and $T_o(z) = T_i + Az^{\lambda}$

(c) $T_i(z) = T_o + A(H - z)^{\lambda}$ and $T_o(z) = T_i + A(H - z)^{\lambda}$

(d) $T_i$ isothermally hot and outer wall subjected to convective boundary condition.

where A = constant, $\lambda$ = power index, $H$ = height of the porous medium

The solution for equations (3.1) is obtained by iteration, yielding the steady state temperatures at all nodes. The mean Nusselt number at the cold wall is calculated using the equation

$$\overline{Nu} = \frac{\int \frac{\partial T}{\partial r} \partial z}{(\Delta T)\frac{H}{L}} \tag{3.24}$$

The temperature gradient $\frac{\partial T}{\partial r}$ at each wall node is obtained by using four point polynomial fit.

# Chapter 4 RESULTS AND DISCUSSION

## 4.1 Inner wall is warm isothermally

Many of the applications of porous medium in engineering involve transmission of fluids through pipes, vessel whereas the walls of fluid can be hotter. For this reason, studies have been carried out for this case where the inside wall of the cylindrical porous annulus is maintained at $T_i$ isothermally. The outside wall is considered at temperature $T_o$ isothermally where $T_i > T_o$. The remaining top and bottom horizontal walls are considered as adiabatic.

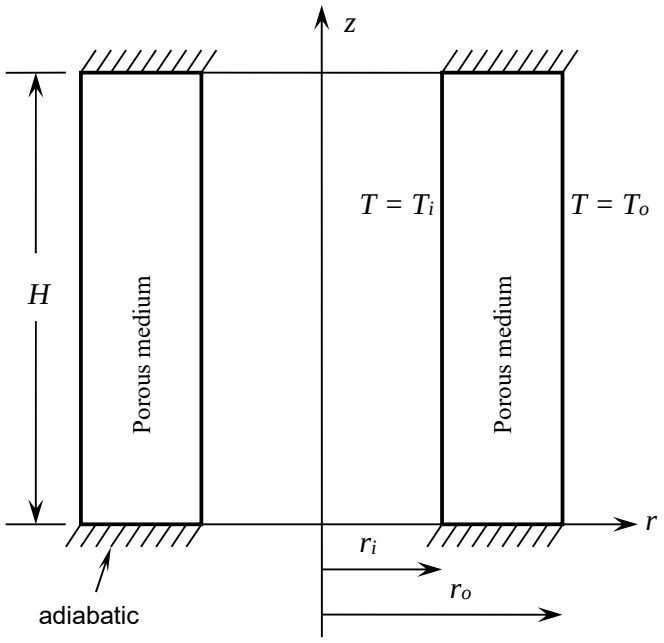


With the aspect ratio and radius ratio fixed as one, the isothermal line and streamline pattern changes depending on different Rayleigh number. Figure 4.1 shows the isothermal lines and streamlines of the porous medium at various Rayleigh numbers. Figure 4.1(a) shows the convection effect is low for low Rayleigh number. The isothermal lines are almost parallel due to low fluid motion to convey the heat. But when the Rayleigh number increases from 50 and 100, the effect can be clearly noticed from Figure 4.1(b) and (c) where the temperature difference near the bottom of the inside wall and top of the outside wall is much greater. It indicates the convection effect is taking place due to the motion of the fluid. As can be seen from the streamlines, the fluid flow for higher Rayleigh number is increases gradually. Because of the greater fluid motion, the isothermal lines deviate more

to the right at the upper portion of the porous medium and deviate to the left at the bottom portion.

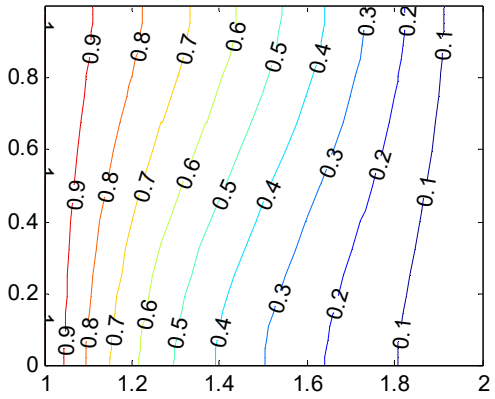

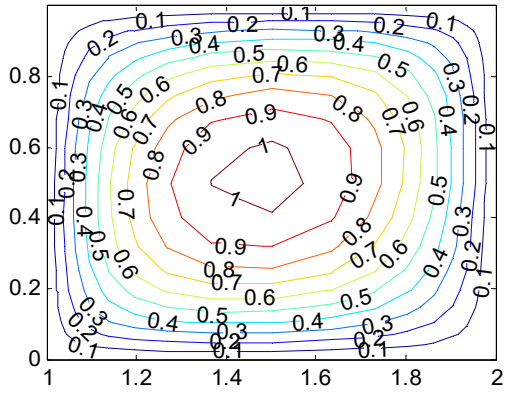

4.1(a) $Ra = 10$

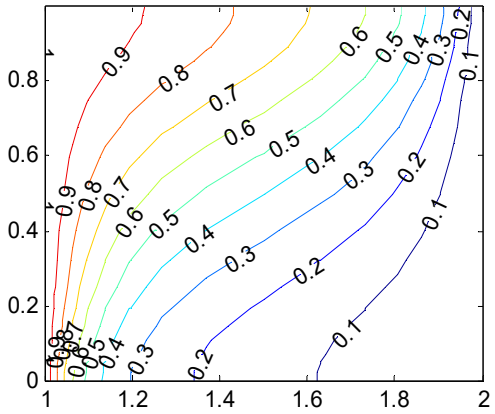

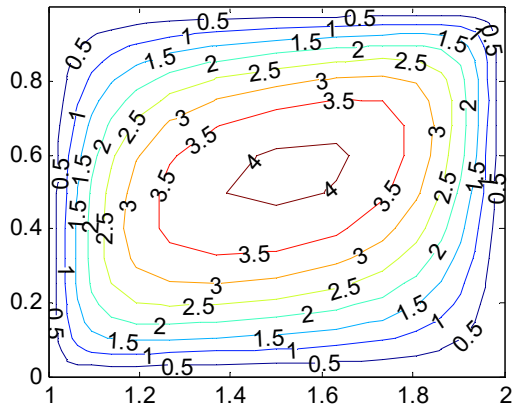

4.1(b) $Ra = 50$

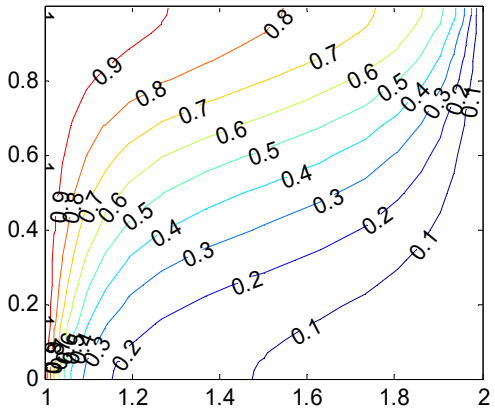

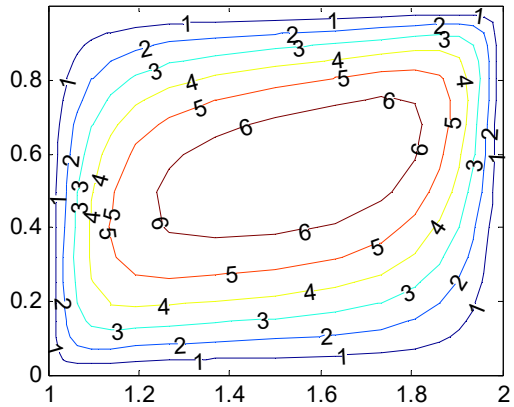

4.1(c) $Ra = 100$

**Figure 4.1**: Isothermal lines (left) and streamlines (right) for $Ra$=10, 50 and 100 with $A^* = r^* = 1$

The study for various aspect and radius ratios has also been taken. It is seen in Figure 4.2 that for constant radius ratio, the average Nusselt number $\overline{Nu}$ increases to reach optimum at aspect ratio of around 1.5 and drops linearly as the aspect ratio increases. In case of higher Rayleigh number $Ra$, the $\overline{Nu}$ is higher as seen in Figure 4.2, the peak of the curves shift towards lower aspect ratio. Figure 4.3 and 4.4 show the isothermal lines and streamlines for different aspect ratios at Rayleigh number of 10 and 100. For low Rayleigh number, the fluid flow is low even as the aspect ration increases; while at high Rayleigh number of 100, the effect of convection is identical greater. The streamline values for $Ra$=100 is higher which indicates the high fluid flow in the porous medium.

As the Rayleigh number increases, the streamlines are concentrated near the bottom of the inside wall and upper of the outside wall, indicating a greater fluid motion because high heat transfer occurs in this area. Due to this high motion of fluid, the isothermal lines converge near the upper and lower horizontal walls and higher temperature difference is seen. This is hardly noticed for low Rayleigh number.

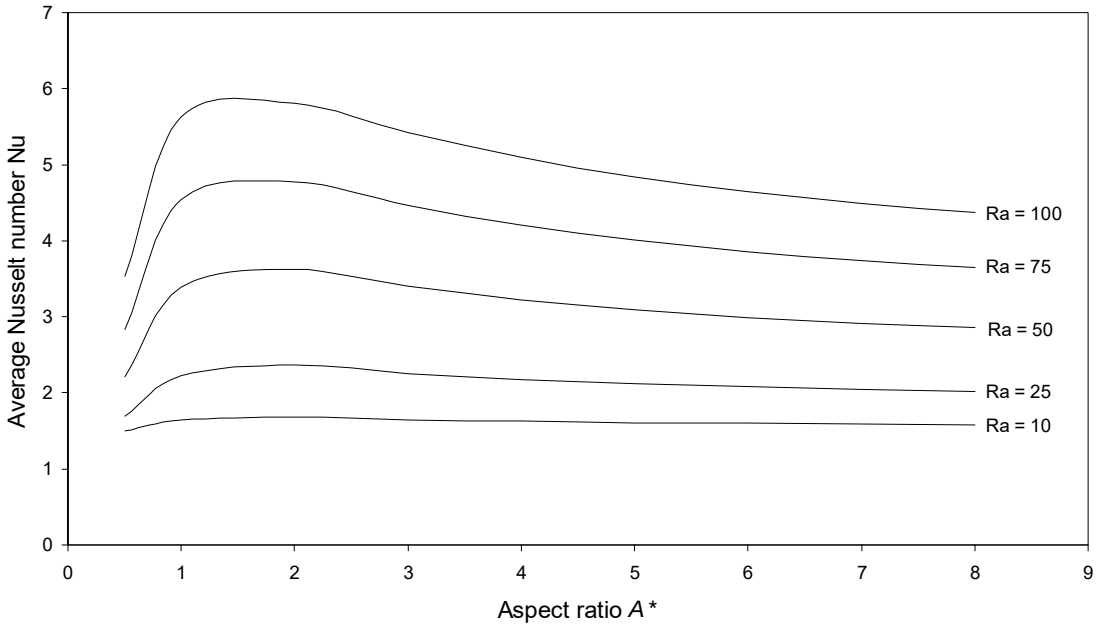


**Figure 4.2**: The variation of $\overline{Nu}$ for different aspect ratio $A^*$ with $r^* = 1$

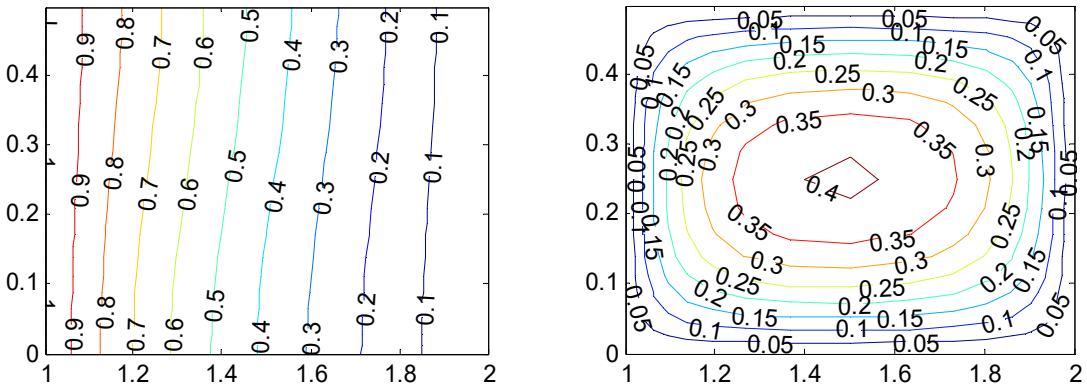

4.3(a) $A^* = 0.6$

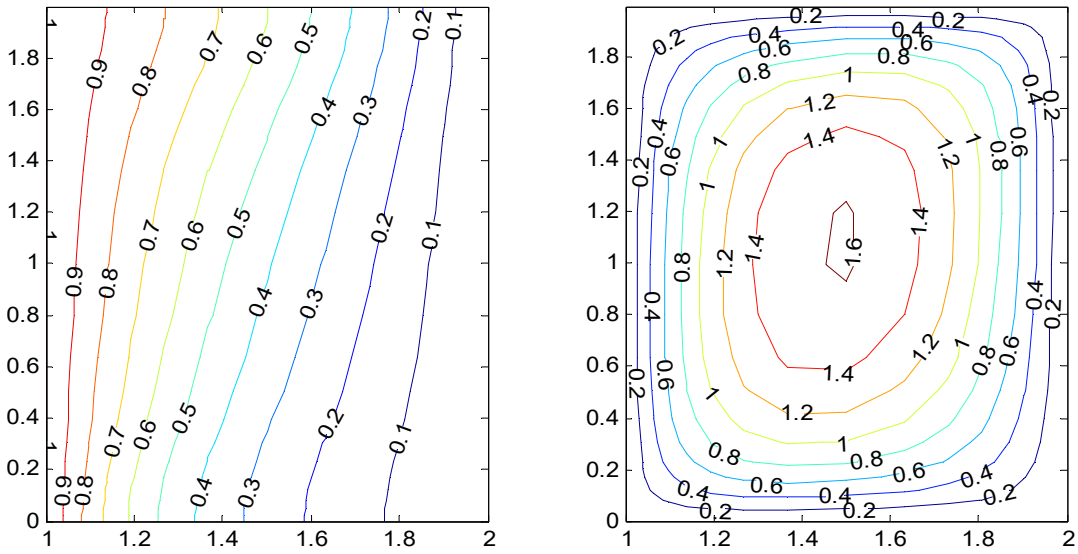

4.3(b) $A^* = 2$

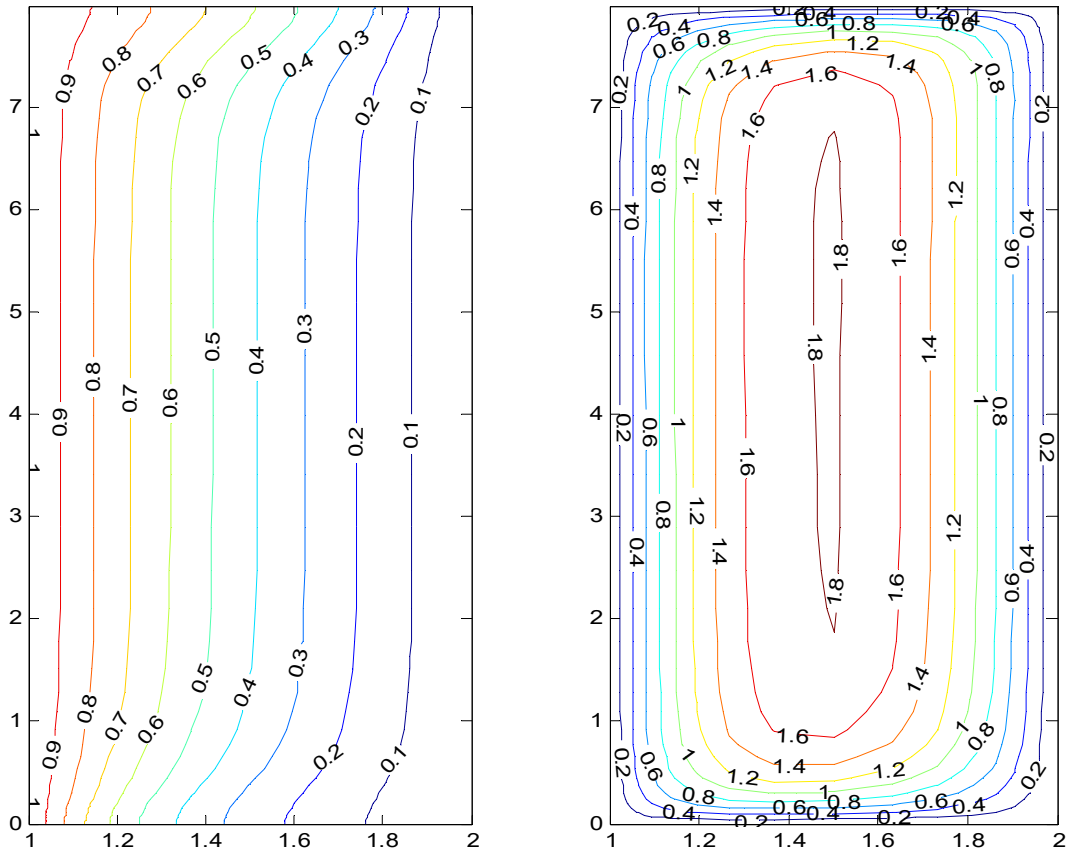

4.3(c) $A^* = 8$

**Figure 4.3**: Isothermal lines (left) and streamlines (right) for aspect ratio of 0.6, 2 and 8 at $Ra$=10 with $A^* = 1$

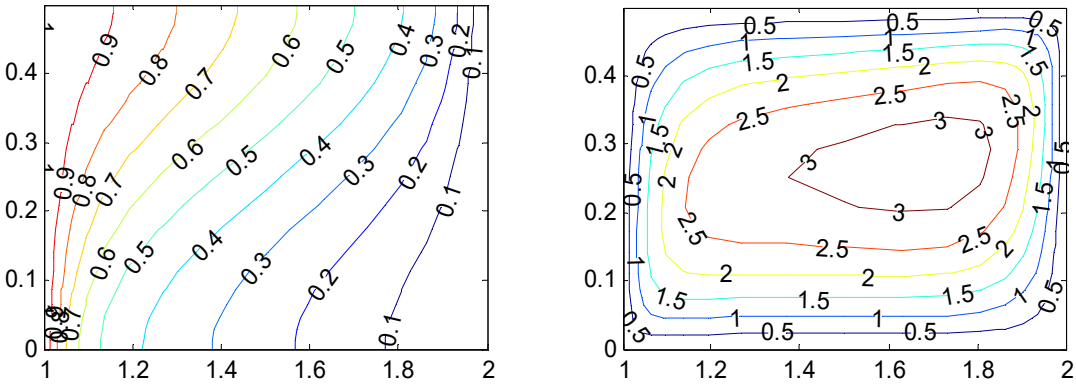

4.4(a) $A^* = 0.6$

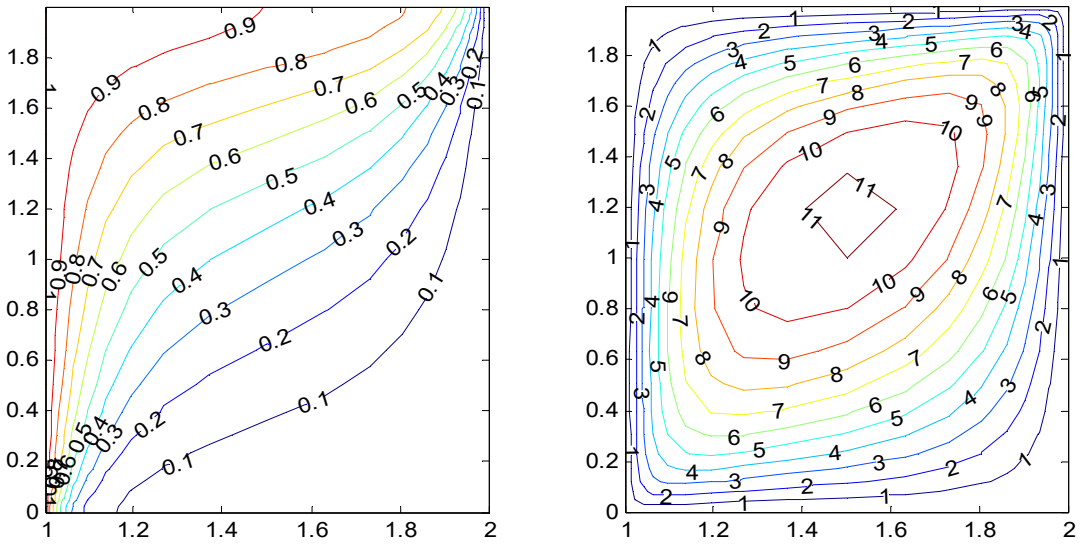

4.4(b) $A^* = 2$

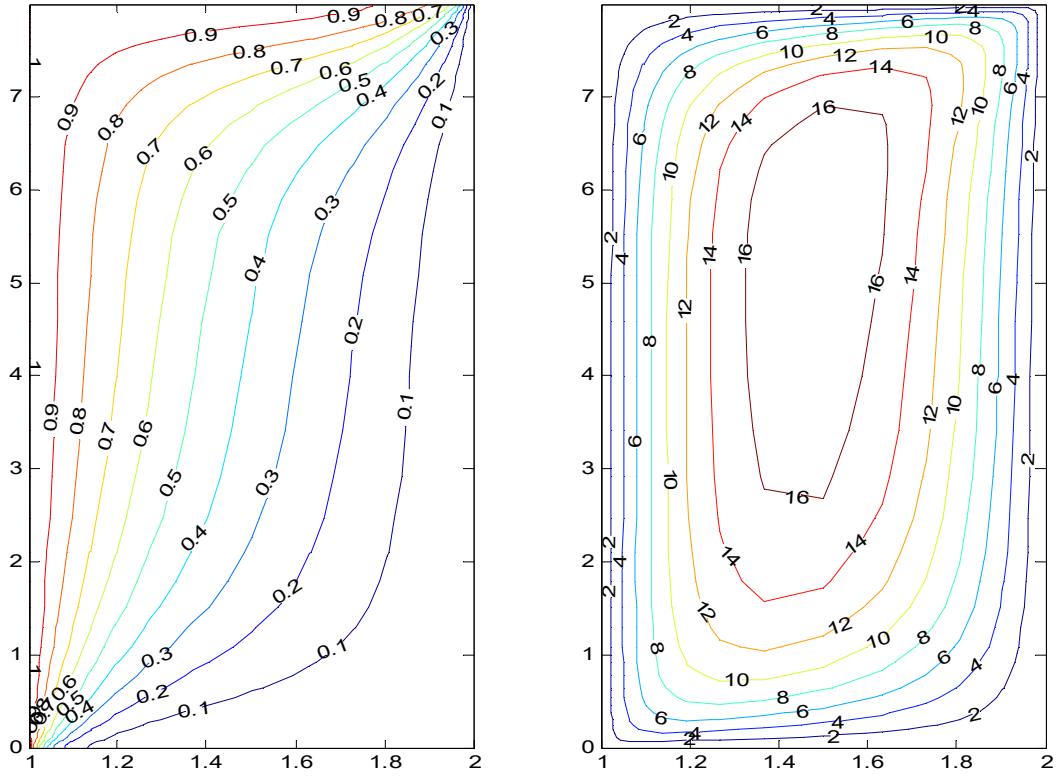

4.4(c) $A^* = 8$

**Figure 4.4**: Isothermal lines (left) and streamlines (right) for aspect ratio of 0.6, 2 and 8 at $Ra$=100 with $r^* = 1$

In the case with constant aspect ratio, the $\overline{Nu}$ always increases with the increment of the radius ratio. From Figure 4.5, as the inverse of radius ratio increases, the $\overline{Nu}$ drops and reaches almost constant value. This shows the radius ratio is dominant than the aspect ratio, for which the $\overline{Nu}$ is much higher when compared with the maxima $\overline{Nu}$ with the aspect ratio of 1.5 for constant radius ratio. Figure 4.7 and 4.8 show the changes of isothermal lines and streamlines when the Rayleigh number increases from 10 to 100. The radius ratio affects the convection greatly, as seen in Figure 4.7 and Figure 4.8 shows high temperature gradient and convection effect occur when the radius ratio is high (annulus thickness is less). At *Ra*=10, the conduction is much dominant, because the isothermal lines are approximately parallel to the walls. As seen, when the radius ratio increases, meaning the inner radius decreases, the heat transfer by convective process becomes predominant.

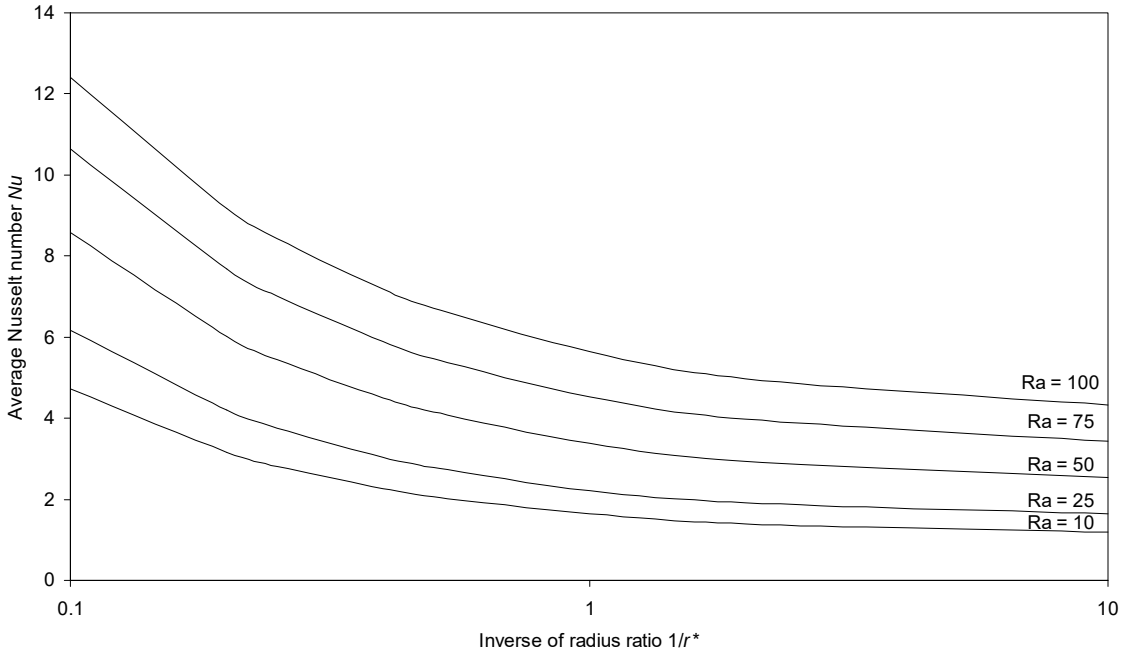


**Figure 4.5**: The variation $\overline{Nu}$ for different inverse radius ratio with $A^*$= 1

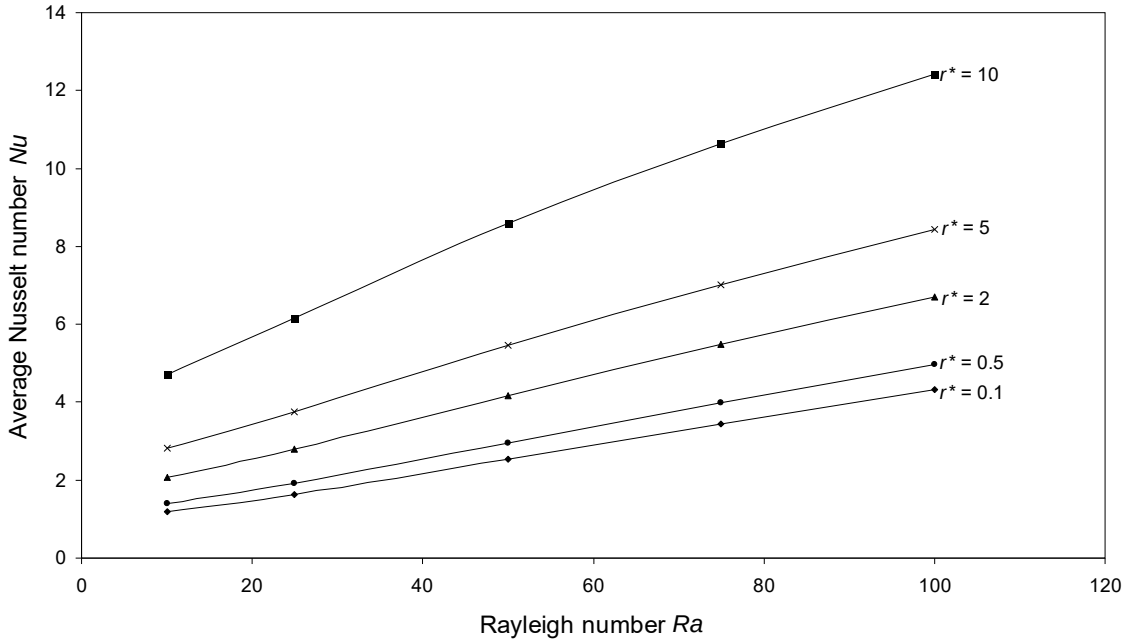


**Figure 4.6**: The variation $\overline{Nu}$ for different *Ra* values with $A^*$= 1

The variation of average Nusselt number for different Rayleigh number is shown in Figure 4.6. This plot is obtained based on the variation of radius ratio from 0.1 up to 10. The aspect ratio is fixed as unity, whereas the inner radius varies according to radius ratio values. As mentioned earlier that when the inner radius decreases, heat transfer by convective process become important and will be a major contributor. From Figure 4.6, the average Nusselt number increase slightly with increment of radius ratio from 0.1 to 10. By increasing the Rayleigh number, the average Nusselt number increase to around 12 at *Ra* = 100 with *r** = 10. The pattern of the lines are almost linear.

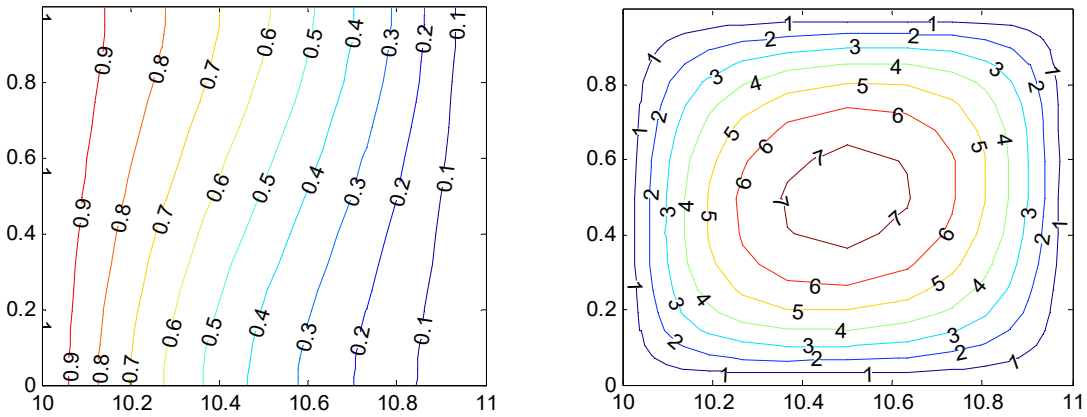

4.7(a) $r^* = 0.1$

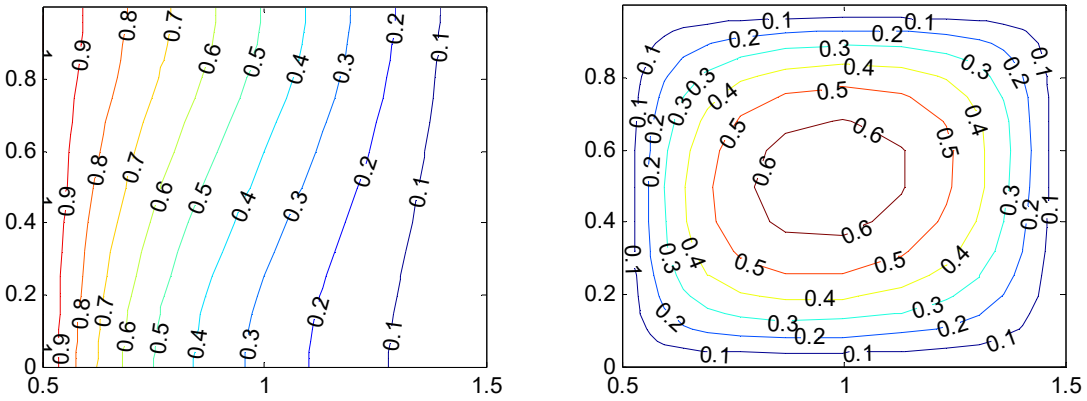

4.7(b) $r^* = 2$

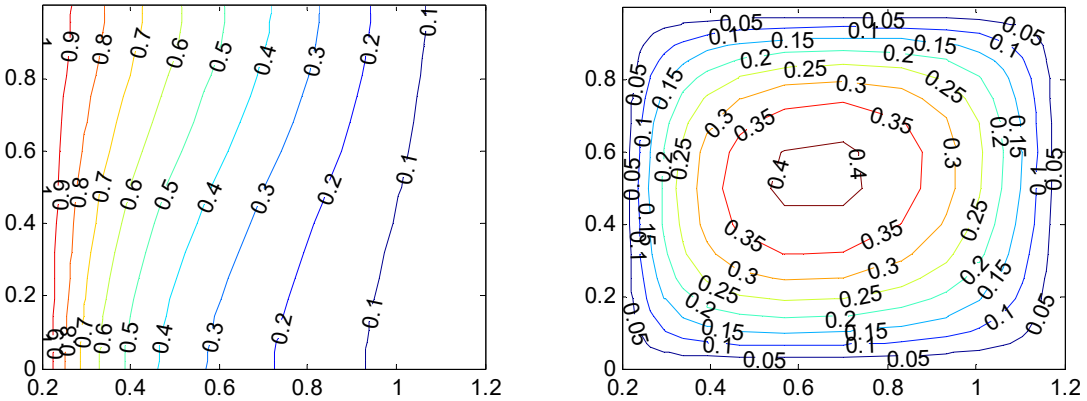

4.7(c) $r^* = 5$

**Figure 4.7**: Isothermal lines (left) and streamlines (right) for radius ratio of 0.1, 2 and 5 at Ra=10 with $A^* = 1$

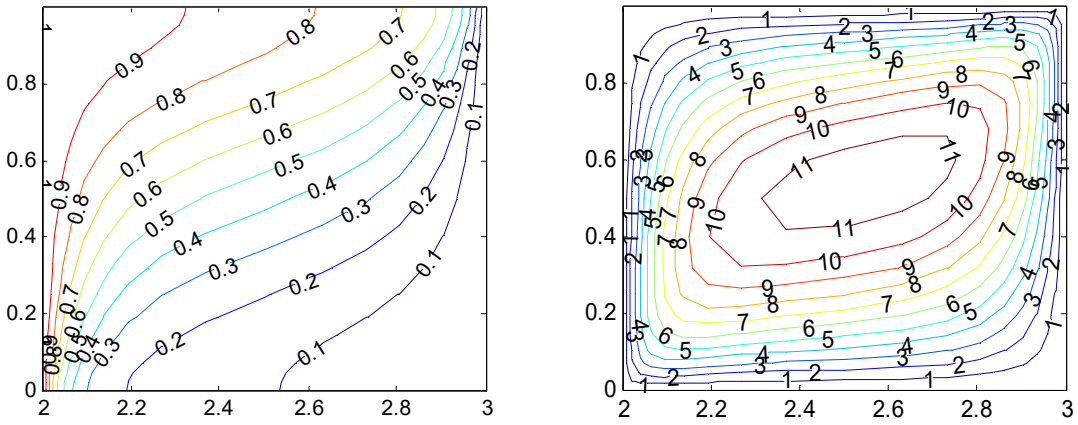

4.8(a) $r^* = 0.1$

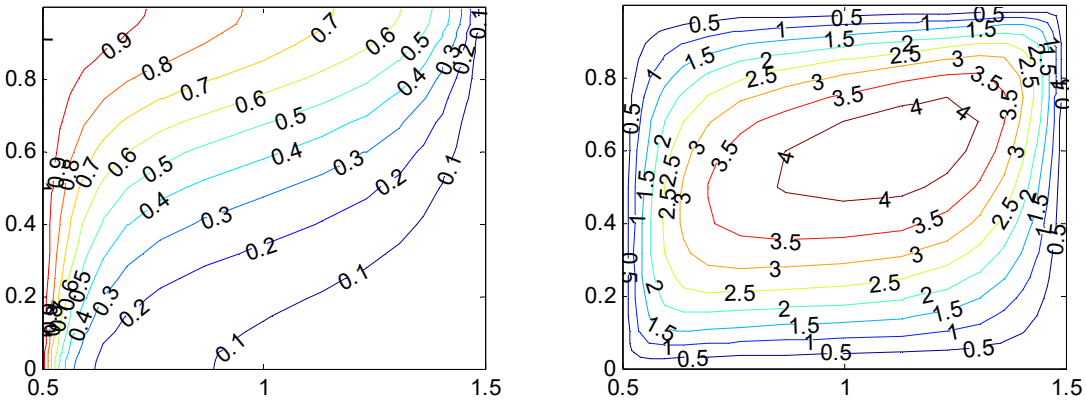

4.8(b) $r^* = 2$

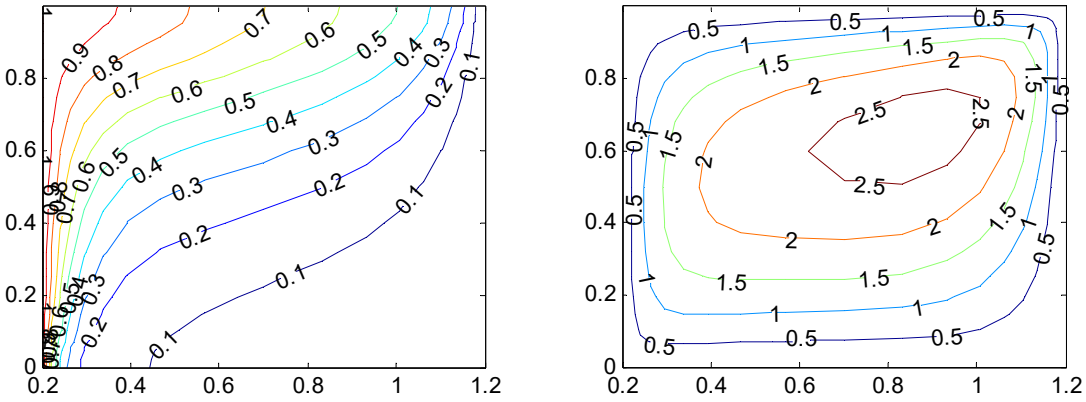

4.8(c) $r^* = 5$

**Figure 4.8**: Isothermal lines (left) and streamlines (right) for radius ratio of 0.1, 2 and 5 at Ra=100 with $A^* = 1$

## 4.2 Power law variation for wall temperature

Here the situation when the wall temperature $T_w$ is a function of distance along the wall has been considered. Four cases have been investigated for this power law wall temperature, which include the outside and inside walls where the temperature may increase from cold to hot or vice versa. The other side of the wall is maintained at isothermally cold. For each of the case, the temperature of the wall is varying by the power index of $\lambda$ = 0.25, 0.50, 0.75 and 1.00. Also the effect of varying the aspect ratio, radius ratio, and power law index along the wall has also been investigated.

### 4.2.1 Power law temperature on the outside wall increasing from $T_i$ at the bottom

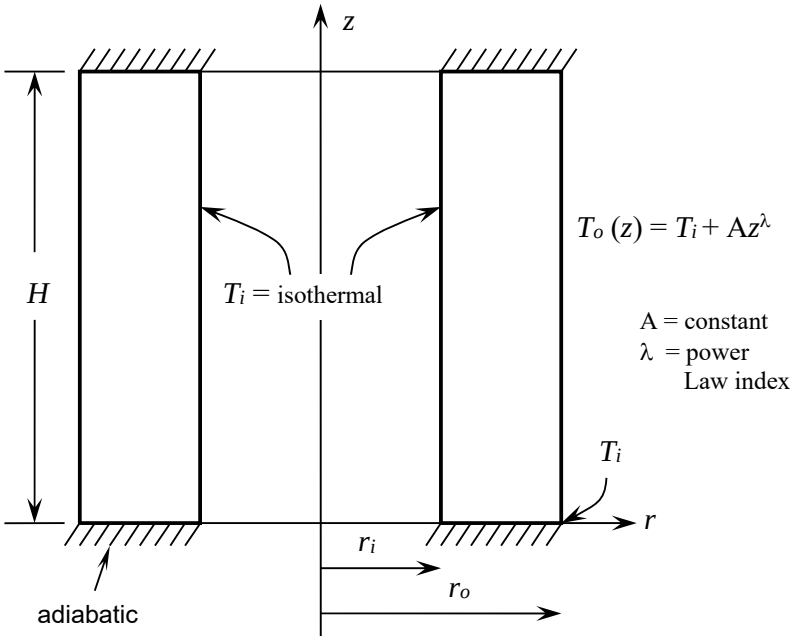


The effect of the power law temperature distribution along the outside wall with the radius ratio being held constant can be seen from the Figure 4.9. For *Ra*=10, the $\overline{Nu}$ increases uniformly while the power law index decrease from 1.00 to 0.25. It shows the $\overline{Nu}$ is different as the aspect ratio is increasing (Figure 4.9(a)). While at higher Rayleigh number of 100, $\overline{Nu}$ increase until its maximum value (aspect ratio = 2.5) and remain constant at its

maximum as the aspect ratio increase. But for the case of λ = 0.25, the $\overline{Nu}$ drops before it remain constant. The inference is that for smaller the power law index, λ, the greater $\overline{Nu}$ will be obtained.

By taking the isothermal lines along the wall into consideration from Figure 4.2, it is seen that $\overline{Nu}$ drops as aspect ratio increases. However it is seen that this type of distribution occur for λ = 0.25 and for other power law index, the value remain almost constant.

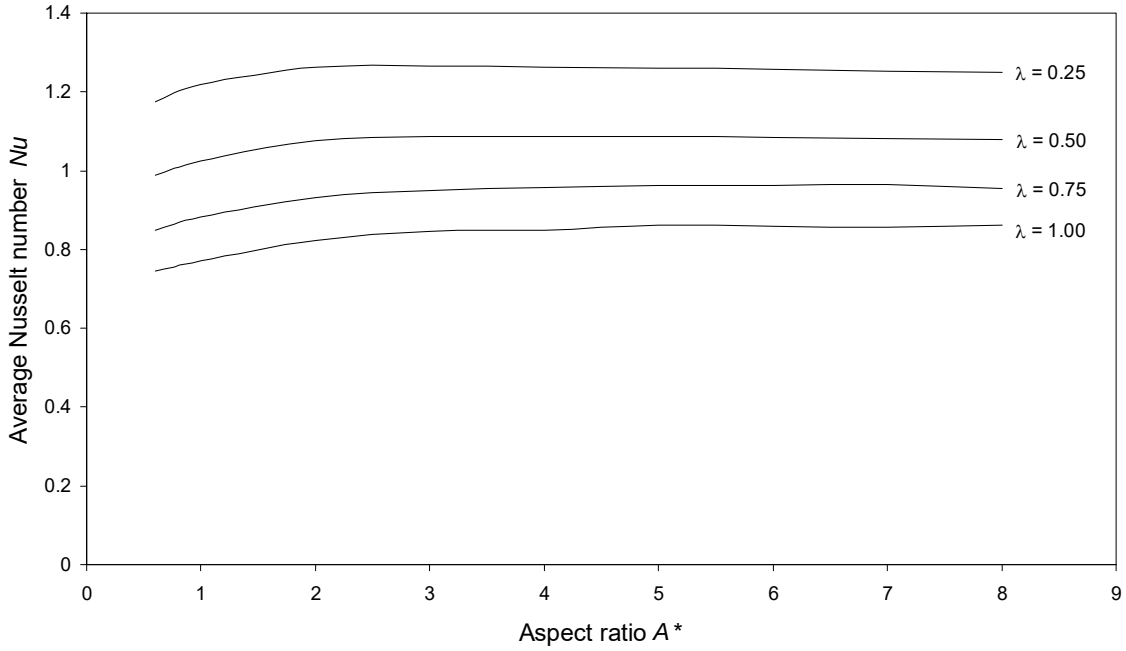


4.9(a) $Ra = 10$

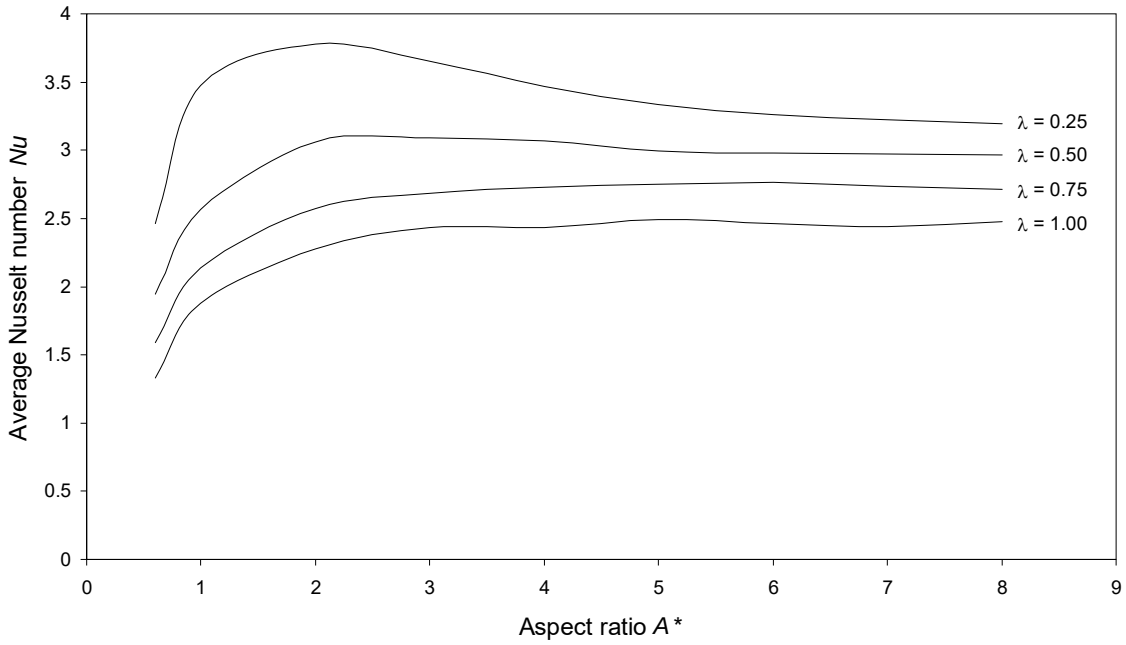


4.9(b) $Ra = 100$

**Figure 4.9**: Variation of $\overline{Nu}$ for various aspect ratios with different power index for $Ra$=10 and $Ra$=100, $r^* = 1$

For different radius ratio at constant aspect ratio, as shown in Figure 4.10(a) and (b), the $\overline{Nu}$ decrease in a similar pattern as the power law index increase from λ = 0.25 to λ = 1.00 when the radius ratio increase. When the radius ratio is low (annulus thickness is large), the $\overline{Nu}$ is very low, about 0.5 – 2, even for the λ = 0.25, the $\overline{Nu}$ is low, indicating that the heat transfer by convection is low when the inner radius of the axisymmetric porous medium is very much greater than the thickness of the porous medium.